2015 2nd International Conference on Mechanics and Mechatronics Research (ICMMR2015)
June 11-12, 2015, Kuala Lumpur, Malaysia

Laser-Inertial Aided 3D Scanner Using Geometric Invariant for Terrain Construction

M.S. Hendriyawan Achmad[1,a], Mohd Razali Daud[2,b], Dwi Pebrianti[3,c], Saifudin Razali[4,d]

[1,2,3,4]Faculty of Electrical & Electronics Engineering, Universiti Malaysia Pahang, Pekan, Malaysia

[a]hendriyawanachmad@gmail.com, [b]mrazali@ump.edu.my, [c]dwipebrianti@ump.edu.my, [d]saifudin@ump.edu.my

Keywords: 3D scanner, geometric invariant, Hokuyo URG-04LX, IMU sensor, complementary filter, gaussian filters.

Abstract. Researchers in robotic vision technology are facing larger challenges, where the 2D technology has flaws in complex robot navigation in 3D space. Using 3D scanner, the robot is able to get a more detailed terrain construction, making it easier to carry out its tasks. The 3D image is obtained by fusing the Hokuyo URG-04LX and the 6-DOF IMU that consists of acceleration sensor and gyro sensor. IMU sensor outputs are the angle, speed, and position in 3D. Nevertheless, just the value of the angle is used in this study to construct 3D images based on geometric invariant. To reduce the interference in the sensor output, two types of filter are applied; the Gaussian filter used on the output of 2D LRF, while the complementary filter is applied to the output of the IMU sensor. Angle measurement plays an important role in term of geometric invariant for terrain construction. The complementary filter has provided the best angle measurement results with the lowest error on time constant (τ) = 0.475s and sampling time (dt) = 10ms. Thus, the proposed systems have successfully made an obvious 3D image of the terrain in the indoor testing.

Introduction

Researchers in robotic vision technology are facing larger challenges, where the 2D technology has flaws in complex robot navigation. Applying the 3D scanner, the robot is able to make a more detailed terrain construction, making it easier to accomplish its mission. The 3D image is obtained by fusing the Hokuyo URG-04LX and the 6-DOF IMU that consists of acceleration sensor and gyro sensor. IMU sensor outputs are the angle, speed, and position in 3D. However, only the value of the angle is employed in this field to make 3D images using geometric invariant. To filter out the noises at the sensor output, two types of filter are used; the Gaussian filter used at the output of 2D LRF, while the complementary filter is used for the output of the IMU sensor. The proposed schemes have successfully created a valid 3D image according to the indoor testing that has been performed.

The mapping is the most substantial part of the mission of a mobile robot to distinguish various objects in the surrounding environment [1], thus autonomous robot is able to determine maneuverable paths while avoiding obstacles [2]. Many studies on the implementation of 2D navigation for SLAM (Simultaneous Localization and Mapping) to determine the current position of the robot in an area has not been recognized previously [3]. However, concurrent with the advancement of technology, a mobile robot is required to perform more complex tasks; not only simply to avoid obstacles and to recover a way, but also able to measure the dimensions of each bit of the surrounding which is employed in the context of path planning information.

There are many ways to generate a 3D image [4] as the basis for the construction of a 3D map. Experiments that have been done in previous works show how a map is developed using the 2D LRF and the 6-DOF IMU sensor [4-7]. IMU sensors provide 3-axis angle information for a 3D image construction and a 3-axis position data used to build a 3D map.

This paper describes the methods of 3D scanning for terrain construction using the 2D LRF sensor Hokuyo URG-04lx and 6-DOF IMU sensor with geometry invariant calculation.

Hardware Setup

In this experiment, two kinds of sensors are used; LRF URG-04LX used to obtain 2D terrain data [8] and IMU sensor MPU6050 which is composed from the 3-DOF acceleration sensor and 3-DOF gyro sensor used to measure angles [9]. A 3D projection of an object is obtained by combining the output of the scanning angle and the distance for the calculation of the geometry. Figure 1 shows a picture both of it.

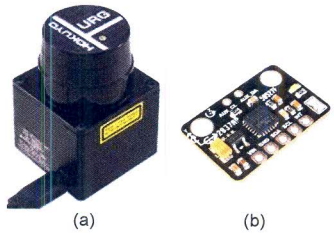

Fig. 1. (a) 2D LRF Hokuyo URG04LX (b) 6-DOF IMU sensor MPU6050

The laser range finder Hokuyo URG04LX measures the distance between 20 to 4095 mm. The measuring coverage angle is 240 points with 682 steps, and then it presents an angular resolution of 0.352 degree. Every scanning period it takes 100 ms, accordingly it will give 10 fps measurement [10]. Since the 2D LRF sensor only capable of scanning in horizontal direction, a tilt mechanism with DC servo motor is applied to enable the laser sensor scanning in vertical direction for 40^0 ranges with 1^0 resolution. Every change in the angle will be measured by the IMU sensors, and employed as input to establish 3D projection. Figure 2 shows scanning method to obtain 3D image.

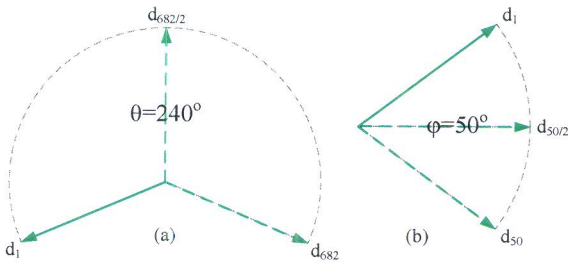

Fig. 2. (a) Horizontal scanning (b) Vertical scanning

Angle values are derived from the fusion process between acceleration sensor and gyro sensor at once as complementary filters that will be spoken about in the succeeding piece. Arduino system is used for IMU sensor data acquisition and to control the DC servomotor of tilt mechanism. Figure 3 shows a diagram of the experimental setup used in this work.

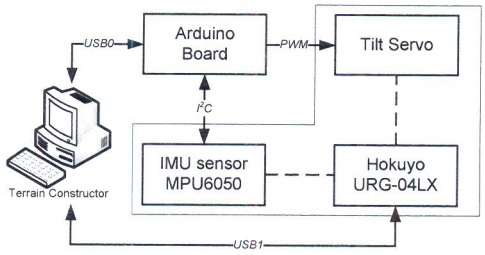

Fig. 3. Schematic diagram of experimental setup

Geometric Invariant

In this study, a geometric invariant plays an important role in the effort to reconstruct the terrain. Geometric invariant contains the distance vectors, with the direction designated by the angle of the vector. Distance vector with its angle are obtained from LRF and IMU sensor. By default, the LRF

Hokuyo URG-04LX produces 682 data with a single 240 degrees left to right horizontal scanning [10]. The outputs are used for 2D projection in the form of polar coordinates (r, θ). To facilitate the required projection in the form of Cartesian coordinates (x, y), Polar into Cartesian conversion needs to be performed. Figure 4 shows coordinate conversion from Polar into Cartesian.

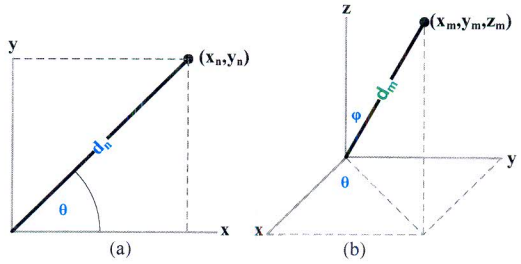

Fig. 4. Polar to Cartesian (a) 2D coordinate (b) 3D coordinate

Polar coordinate involves the azimuth (θ) and distance (d). Azimuth is the angle of the horizontal scan respect to the initial position, with the azimuth (θ) = n*0.352 degree, where n is the sequence number from 1 to 682. Based on Figure 4(a), 2D Polar to Cartesian projection could be established by using Equation (1, 2) below.

$$x_n = d_n \times \cos(\theta). \tag{1}$$

$$y_n = d_n \times \sin(\theta). \tag{2}$$

Where, n is the sequence number from 1 to 682. Thus, 2 matrix (X,Y) are obtained, as shown by equation (3,4).

$$X_{2d} = [x_1, x_2, x_3, ..., x_{682}]. \tag{3}$$

$$Y_{2d} = [y_1, y_2, y_3, ..., y_{682}]. \tag{4}$$

Based on Figure 4(b), Z axis is needed in addition to the X axis and Y axis, to build a 3D image. To obtain the value of Z, vertical scanning of depth is required for each inclination angle (φ) in the 40 degree range. Inclination angles (φ) are obtained from IMU sensor, which will be discussed in the next section. Equations (5-7) show the conversion steps from polar-spherical to 3D cartesian coordinates.

$$x_m = d_m \times \cos(\theta) \times \sin(\varphi). \tag{5}$$

$$y_m = d_m \times \sin(\theta) \times \sin(\varphi). \tag{6}$$

$$z_m = d_m \times \sin(\theta) \times \cos(\varphi). \tag{7}$$

Where, m is the sequence number from 1 to 682. Thus, 2 matrix (X,Y) are obtained, as shown by equation (8-10).

$$X_{3d} = [x_1, x_2, x_3, ..., x_{682}]. \tag{8}$$

$$Y_{3d} = [y_1, y_2, y_3, ..., y_{682}]. \tag{9}$$

$$Z_{3d} = [z_1, z_2, z_3, ..., z_{682}]. \tag{10}$$

Output Denoising

Sensors output could be disturbed by noise that are triggered by many sources from inside or outside. This work uses two kinds of filter. Complementary filter is applied to the outputs of the IMU

sensor (Acceleration and gyro) to perform fusion function, while 1D Gaussian filter is applied to the LRF Hokuyo URG04LX output to perform a smoothing function.

Complementary Filter – The complementary filter does not take into account any statistical description about the noise which is distracting the signals, and it is performed by simple analysis in the frequency domain [11]. This filter performs complementary method to the output of acceleration and gyro sensor. Between acceleration and gyro sensor have different characteristic in term of their response to the input. Acceleration sensor measure all forces not only from the gravity vector alone, and easily distracted even with small force. Data from the acceleration sensor only reliable in the long term and the most appropriate filter is a low pass filter to remove noise on acceleration sensor. Gyro sensor measures angular velocity and less affected by external force, but the drift will always produce the result that cannot go to zero when the system returns to its original position. Complementary filter utilizes the advantages from both the sensors. For the short term, this filter uses the data from the gyroscope, because it is very precise and not susceptible to external forces. For the long term, this filter uses the data from the accelerometer, as it does not drift. Figure 5 shows diagram of Complementary filter.

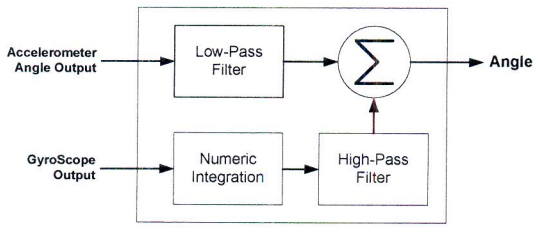

Fig. 5. The diagram of Complementary filter

Based on Figure 5, diagram of complementary filters can be poured into the form of discrete mathematical equations, shown by equation 11.

$$Angle = (\alpha) \times (Angle + Gyro_{output} \times dt) + (1 - \alpha) \times (Angle_{accel\_output}). \quad (11)$$

Where α is the filter coefficient that determines the weighting of the input to the output, it's determined by time constant (τ) and sampling time (dt) as shown by equation 12. $Gyro_{output}$ is an angular speed which was measured by gyroscope, and $Angle_{accel\_output}$ is an angle which was calculated based on acceleration changing by using ATAN function.

$$\alpha = \frac{\tau}{\tau + dt}. \quad (12)$$

$$\tau = \frac{\alpha \times dt}{1 - \alpha}. \quad (13)$$

Where, the time constant (τ) can be assumed as the boundary between trusting the gyroscope, and trusting the accelerometer. By changing the value of the time constant will determine the characteristics of the filter response, in other words it will change the cut off frequency of HPF and LPF. Sampling time (dt) means a period where the IMU sensor will be read constantly. In this work, the sampling time is 10milisecond. In opposite, equation 13 shows how to find out desired time constant respect to α which has been known.

Gaussian Filter – This filter is commonly known in image processing for denoising purposes [12]. In this work, it is used to maintain the output of LRF sensor. In contrast to the 2D image smoothing method that uses a two-dimension Gaussian filter, this work used a one-dimension Gaussian filter only. However, it is applied to every horizontal scan output of LRF sensor. In mathematics, the 1D gaussian filter is written as shown by equation 14.

$$G(x) = \frac{1}{\sqrt{2\pi\sigma^2}} e^{-\left(\frac{x^2}{2\sigma^2}\right)}. \tag{14}$$

Where, σ is the standard deviation of the distribution. The distribution is assumed to have a mean (μ) of 0.

Result & Discussion

Polar to Cartesian Conversion – LRF sensors Hokuyo URG-04LX has an output in the form of a 2D polar coordinate, it needs to be converted into 2D Cartesian coordinate using equation 1 and 2. Figure 6 shows the projections of a 2D LRF data acquisition.

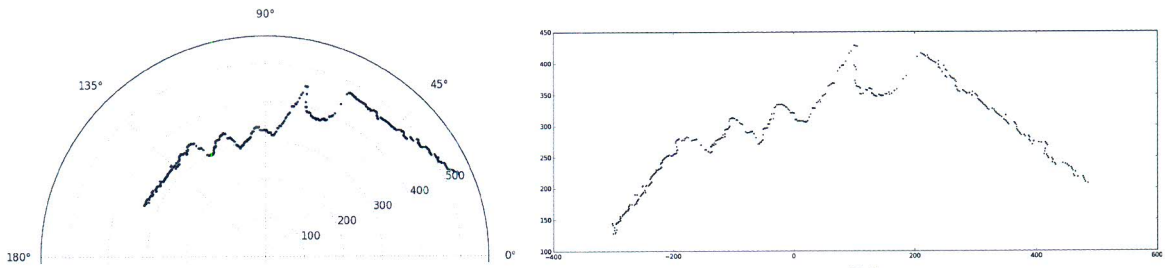

(a) (b)

Fig. 6. 2D projection (a) Polar plot (b) Cartesian plot

Angle Measurement – The value of the angle is obtained from the output of the complementary filter based on the calculation indicated by equation 11. This experiment using the sampling time (dt) 10 ms while a time constant (τ) is variable. And then observe the influence of the time constant (τ) against errors of measurement. Input parameters and experimental results are shown in the Table 1 below.

Table 1. Complementary Filter Error Result

	Complementary filter parameters			
Objective	τ_1 = 0.4s dt = 0.01s	τ_2 = 0.45s dt = 0.01s	τ_3 = 0.475s dt = 0.01s	τ_4 = 0.5s dt = 0.01s
Mean	-4.378	-1.166	-0.74	-2.731
Stdev	6.506	1.138	0.708	4.278

In this experiment, measurement are taken from 40 deg to 90 deg with the number of samples are 15. Then, they are compared with manually measured data. The measured data are presented in terms of Mean and Standard Deviation. The experiment is carried out for each variable of Time Constant (τ), i.e. 400 ms, 450 ms, 475 ms, and 500 ms. Figure 7 shows the statistical description of angle measurement based on Table 1.

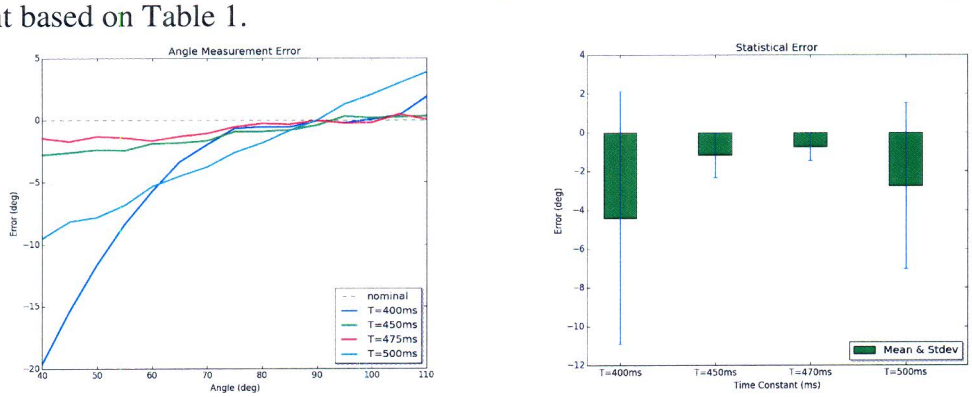

Fig. 7. Error of Angle Measurements

Figure 7 shows the fact that the complementary filter has provided the best angle measurement results as it known to have the lowest error when time constant (τ) = 0.475s and sampling time (dt)=10ms.

Smoothing Function – Noises at the output of LRF sensor are uneasy to reject, and it is stoutly influenced by the surfaces feature of the observed object, such as color and reflectivity of the light [13][14]. The smoothing function to the output of the LRF sensor is necessary for this problem. Gaussian filter is used in this work. Equation 14 shows the mathematical functions from the 1D Gaussian filter. Figure 8 shows the results of smoothing function using 1D Gaussian filter for the value of $\sigma = 3$ and $\sigma = 6$.

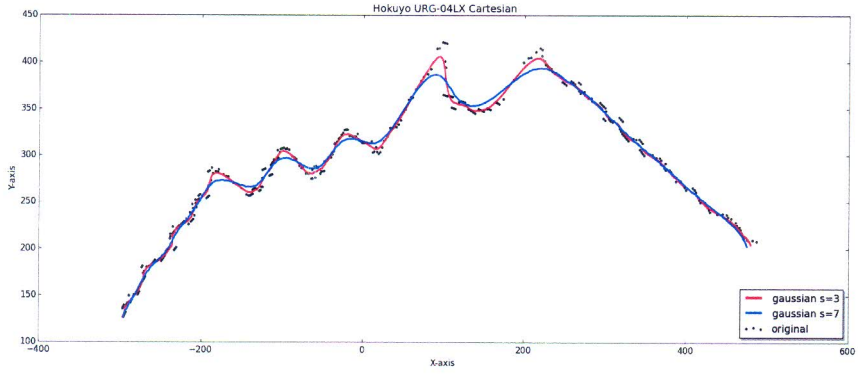

Fig. 8. 1D Gaussian Filter Performance

Based on the figure 8, with the value of $\sigma = 3$ has provided the result close to the actual contour with reduced noise. Compared with the value of $\sigma = 7$, even though the result has less noise, but the constructed contour has bigger different compared to actual.

Terrain Construction – In order to construct 3D contour of the terrain, the combination of horizontal and vertical scan is carried out. Then, equations (5-7) are applied to each input distance (d) and angles (θ, φ). Complementary filters ensure proper readability of vertical scan angles (φ), whereas the Gaussian filter discards the noises from LRF output caused by uncertainty factor of the object's surfaces. Figure 9 shows the final results of this work.

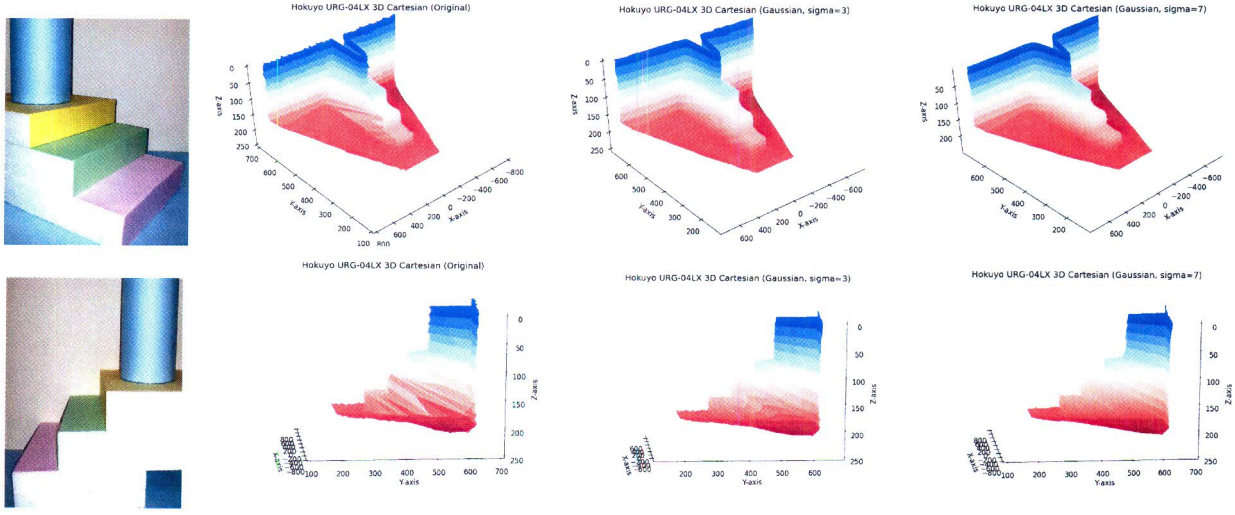

(a) (b) (c) (d)

Fig. 9. 3D Terrain Construction (a) Original Image (b) Original 3D Construction (c) Gaussian Smoothing with $\sigma = 3$ (d) Gaussian Smoothing with $\sigma = 7$

This paper presents a method of 3D image construction using 2D LRF Hokuyo URG-04LX sensor with the tilt servo mechanism. The correction of tilt angle of the mechanism is done by the IMU MPU6050 sensor. Filtering process was carried out to eliminate noise (denoising) on the both of the outputs of the IMU sensors and LRF sensor. Complementary filter plays an important role providing angle information accurately. It provides the best angle measurement results with the lowest error when the time constant (τ) = 0.475 sec and sampling time (dt) =10 ms. In this work, LRF sensor output is smoothed using a 1D Gaussian filter. Obviously, the results which are shown in Figure 10 proved that the terrain has been well constructed and can be used for robotic 3D vision.

Acknowledgement

This project is supported by Malaysian Ministry of Higher Education under Exploration Research Grant Scheme, ERGS, RDU130604.

References

[1] D. F. Wolf, G. S. Sukhatme, and S. Member, "Semantic Mapping Using Mobile Robots," *IEEE Trans. Robot.*, vol. 24, no. 2, pp. 245–258, 2008.

[2] C. Chen and Y. Cheng, "Research on Map Building by Mobile Robots," *IEEE - Second Int. Symp. Intell. Inf. Technol. Appl.*, pp. 673–677, Dec. 2008.

[3] B. B. Cortes, U. Valle, B. Piv, and X. C. Solé, "Indoor SLAM using a Range-Augmented Omnidirectional Vision," in *IEEE International Conference on Computer Vision Workshops*, 2011, pp. 280–287.

[4] M. Bosse, R. Zlot, and P. Flick, "Zebedee : Design of a Spring-Mounted 3-D Range Sensor with Application to Mobile Mapping," *IEEE Trans. Robot.*, vol. 28, no. 5, pp. 1104–1119, 2012.

[5] S. Oßwald and A. Hornung, "Autonomous Climbing of Spiral Staircases with Humanoids," *IEEE/RSJ Int. Conf. Intell. Robot. Syst. Sept. 25-30. San Fr. CA, USA*, pp. 4844–4849, 2011.

[6] Y.-S. Hawng, K. Hyun-Woo, and J.-M. Lee, "A 3D Map building algorithm using a single LRF on a mobile robot," in *9th International Conference on Ubiquitous Robots and Ambient Intelligence (URAI), November 25-29, Daejeon, Korea*, 2012, vol. 1, pp. 321–324.

[7] D. Magree and E. N. Johnson, "Combined Laser and Vision-aided Inertial Navigation for an Indoor Unmanned Aerial Vehicle," in *American Control Conference (ACC) June 4-6. Portland, Oregon, USA*, 2014, pp. 1900–1905.

[8] H. Kawata, A. Ohya, S. Yuta, W. Santosh, and T. Mori, "Development of ultra-small lightweight optical range," in *IEEE International Conference on Intelligent Robots and Systems (IROS)*, 2005, no. 42 50, pp. 1078 – 1083.

[9] InvenSense, "MPU-6000 and MPU-6050 Product Specification Rev 3.4," 2013.

[10] M. Ogaz, R. Sandoval, and M. Chacon, "Data Processing from a Laser Range Finder Sensor for the Construction of Geometric Maps of an Indoor Environment," in *Midwest Symposium on Circuits and Systems*, 2009, pp. 306–313.

[11] W. T. Higgins, "A Comparison of Complementary and Kalman Filtering," vol. 1975, no. 3, pp. 321–325, 1975.

[12] Y. Huang and G. Qu, "A New Image Restoration Method by Gaussian Smoothing with L 1 Norm Regularization," in *5th International Congress on Image and Signal Processing (CISP)*, 2012, no. Cisp, pp. 343–346.

[13] L. Kneip, F. Tache, G. Caprari, and R. Siegwart, "Characterization of the compact Hokuyo URG-04LX 2D laser range scanner," in *IEEE International Conference on Robotics and Automation*, 2009, pp. 1447–1454.

[14] Y. Okubo, C. Ye, and J. Borenstein, "Characterization of the Hokuyo URG-04LX Laser Rangefinder for Mobile Robot Obstacle Negotiation," 2009, vol. 7332, pp. 1–10.